

Transitioning late-time cosmology with the Hubble parameterization

Vinod Kumar Bhardwaj*

Department of Mathematics, GLA University, Mathura 281406, Uttar Pradesh, India

Saibal Ray†

*Centre for Cosmology, Astrophysics and Space Science,
GLA University, Mathura 281406, Uttar Pradesh, India*

Kazuharu Bamba‡

Faculty of Symbiotic Systems Science, Fukushima University, Fukushima 960-1296, Japan

Akram Ali§

*Department of Mathematics, College of Sciences,
King Khalid University, Abha 61413, Saudi Arabia*

Abstract

We investigate a late-time cosmological model for a homogeneous and isotropic space-time in the Rastall theory. We explore the observational constraints on the Hubble parameter by using the latest cosmological datasets such as cosmic microwave background radiation (Planck), baryon acoustic oscillations (DESI) and Type Ia Supernovae (Union 3.0). As a result, we explicitly demonstrate that the specific redshift transition occurs, namely, there happens a phase shift in the evolution of the universe from the initial deceleration era to the current accelerating phase of the cosmological scenario. Furthermore, we show that with the latest dataset of DESI-BAO clubbed with CC, CMB, and Union 3.0, the current value of the Hubble parameter is estimated as $H_0 = 66.9451.094$, which can be compatible with the available observations.

* Email:dr.vinodbhardwaj@gmail.com

† Email:saibal.ray@gla.ac.in

‡ Email:bamba@sss.fukushima-u.ac.jp

§ Email:akali@kku.edu.sa

I. INTRODUCTION

Einstein's General Theory of Relativity (GR) stands as one of the most profound scientific achievements of the twentieth century, establishing a deep relationship between the geometry of spacetime, radiation, and matter. GR has played a pivotal role in describing both the early inflationary epoch and the present as well as future phases of the universe's expansion. Observational results from Cosmic Microwave Background Radiation (CMBR), Wilkinson Microwave Anisotropy Probe (WMAP), Type Ia supernovae (SN Ia), Large Scale Structure (LSS), Baryon Acoustic Oscillations (BAO), Dark Energy Spectroscopic Instrument (DESI), Union 3.0 and so on collectively confirm that the current universe is undergoing accelerated expansion [1–7]. Although cosmological models grounded in GR successfully reproduce many observational results [1–3], the late-time cosmic acceleration poses fundamental questions regarding the GR viability on large scales [8]. This accelerating behavior has been attributed to an unknown component with negative pressure, known as dark energy (DE), which brought back Einstein's cosmological constant Λ as a possible candidate for explaining it [8, 9]. However, despite its success, the Λ CDM framework faces persistent theoretical challenges such as the fine-tuning problem, the cosmic coincidence issue, and the H_0 tension. To overcome these shortcomings, numerous dynamical DE models and modified gravity theories have been introduced, encompassing extra-dimensional and scalar field approaches [10–16].

The equivalence principle forms one of the cornerstones of GR. Nonetheless, certain theoretical and observational considerations indicate that this principle might be violated under specific conditions, which has led to increased interest in alternative gravitational theories that go beyond the framework of General Relativity. The divergence-free energy-momentum tensor (EMT), that interacts weakly with spacetime geometry, plays a fundamental role in constructing GR and its modified versions [17, 18]. However, several works argue that particle creation processes could violate EMT conservation, challenging the standard condition $\nabla_\nu T^{\mu\nu} = 0$ [19–22]. This opens the possibility of formulating gravitational theories where EMT conservation is relaxed. Consequently, modified gravity frameworks [23–25] have become promising tools to address cosmological issues such as the '*dark energy (DE)*' [1, 26] as well as '*dark matter (DM)*' problems [27, 28]. Any such alternative, however, must be consistent with both theoretical and observational constraints. In this direction, various modified theories of gravity have been extensively developed and investigated [29–35].

Among these alternatives, the theory proposed by Peter Rastall in 1972 [36] has gained significant attention. The Rastall theory revisits the conservation law of the EMT, questioning its strict validity in curved spacetime even though it holds in the Minkowski limit or weak-field scenarios. In this framework, the postulate $\nabla_\nu T^{\mu\nu} = 0$ is replaced by a more general condition where the divergence of the EMT is directly proportional to the gradient of the Ricci scalar, i.e., $\nabla_\nu T^{\mu\nu} \propto \nabla^\mu R$. Thus, the Rastall theory introduces a coupling between geometry and matter, where curvature can influence the non-conservation of energy and momentum. This coupling can also be deciphered as an effective interpretation of quantum effects in the Riemannian curved spacetime [37]. The curvature-matter coupling mechanism allows non-minimal interactions between geometry and matter, naturally guiding to a breakdown of the conventional conservation law [38–41]. Recent research has extensively explored different aspects of the Rastall theory, including its implications for DE perturbations [42], its relation with the scalar field of Brans–Dicke theory [43] and its predictions regarding the inner composition of compact stars, especially neutron stars [44]. A number of works have also analyzed different cosmic evolution stages within this theoretical framework, offering valuable observational support and theoretical interpretations [45–49].

Interestingly, the Rastall theory is unrestricted from age and entropy related issues [50] and therefore delivers interpretations for both the inflationary as well as accelerated cosmic expansion [45, 51]. Furthermore, Moradpour et al. [51] argued that the non-minimally coupled interaction in between the pressureless matter part and geometrical fabric of spacetime in the Rastall theory can effectively replicate dark energy behavior, successfully explaining the observed accelerated expansion of the universe. The theory has been tested across different cosmological eras, including the inflationary, matter-dominated, and late-accelerating phases [52]. Moreover, the cosmological model developed in Ref. [53] under the Rastall framework shows convergence with the Λ CDM model at late times, and the inclusion of a Rastall parameter has been suggested as a

possible resolution to the initial singularity problem [52].

It is important to highlight that there exists an ongoing debate about whether the Rastall theory is fundamentally equivalent to General Relativity (GR). While both frameworks share some mathematical and conceptual similarities – particularly in terms of the Energy–Momentum Tensor and the presence of non-minimal coupling – there are also significant distinctions. Hence, certain studies argue in favor of equivalence [54, 55], whereas others support non-equivalence [56–58]. In this work, we treat GR and the Rastall theory as distinct yet interconnected frameworks, considering the Rastall theory within the GR platform to examine cosmological evolution. As demonstrated later (see discussions in connection to Eqs. (2.2) and (2.3)), under a specific constraint on the Ricci scalar R , both theories can coincide.

In the present study, we employ modern *Deep Learning* (DL) techniques – a specialized branch of Machine Learning (ML) – to examine the accelerating expansion phase of the present universe by means of constraining cosmological parameters. Using the `COLFI` Python package [59], we estimate the parameters through Artificial Neural Networks (ANN), Mixture Density Networks (MDN), and Mixture of Gaussian Networks (MNN) [60–63]. These approaches allow conditional probability distributions to be learned directly from observational data while also supporting efficient inference of posterior distributions [59–61]. Additionally, hyper-ellipsoid constraint techniques are employed to improve neural network (NN) training and to achieve more precise parameter estimation [62, 63].

Various experimental findings which include Ia supernovae [64, 65], Cosmic Microwave Background (CMB) [66, 67], Baryon Acoustic Oscillations (BAO) [68, 69], Large Scale Structure (LSS) [70, 71] conclusively confirmed the present era of an accelerating universe (also *vide* Ref. [72] and other references therein). In the present work we therefore perform a comparative assessment of neural network–based techniques against the traditional Markov chain Monte Carlo (MCMC) method to validate the already obtained features of the late time cosmic acceleration. We show that the MNN outcomes are in strong agreement with those obtained from the MCMC method, validating the reliability and effectiveness of the DL approach. The proposed cosmological model successfully reproduces accelerated phase of the present-day universe without invoking an exotic entity, i.e., DE and overcomes the issue of the erstwhile cosmological constant. Thus, the use of observational data within the Rastall theory becomes essential for accurate modeling. Our findings demonstrate that neural network-based estimation provides a powerful substitute to the MCMC approach. The Rastall framework allows investigation of gravitational effects on cosmic expansion through ANN, MNN, and MDN algorithms. This study forms part of a broader research direction integrating cosmology with ML, illustrating how AI techniques can efficiently address complex problems related to cosmic evolution as well as expansion.

The paper is organized as follows: the solution of the Rastall field equations with logarithmic parameterization of $H(z)$ is presented in Sec. II. Sec. III discusses observational constraints on model parameters obtained via three different methods and datasets. Section IV examines the model’s dynamical features, including energy density, pressure, and the deceleration parameter, as well as diagnostic tools like statefinders. The energy conditions governing the model’s physical viability are analyzed in Sec. V. Finally, Sec. VI provides a few essential concluding remarks on this work. In Appendix A, we describe with graphical presentations, the ML technique to estimate the model parameters by utilizing the latest datasets of CMB, BAO-DESI, Union 3.0 etc. whereas in Appendix B, we show the explicit expressions for the statefinder parameters (i.e., r and s).

II. MODEL AND THE FIELD EQUATIONS IN RASTALL’S GRAVITY

Rastall’s gravitational framework stands out as an interesting branch within the family of modified gravity theories [36]. In this work, we are trying to derive feasible solutions by physically considering both the matter sector and the underlying spacetime geometry. It is noteworthy that without maintaining the matter energy–momentum tensor based conservation law, the Bianchi identities hold good in the Rastall theory, and thus leading to a modified condition $T^{ij}_{;i} = \lambda R^{ij}$, where R and λ denote respectively the Ricci scalar and the coupling parameter which is involved in the Rastall theory. Unlike GR, where the conservation equation obeys $\nabla_j T^{ij} = 0$, the more generalized form in the Rastall theory is written

as $\nabla_j T^{ij} = u^i$ [36, 46, 73]. To recover the standard GR conservation law, the vector on the right-hand side must vanish. Accordingly, this vector is defined as u^i is therefore parameterized as $u^i = \lambda \nabla^i R$. The corresponding field equations governing the Rastall theory are established as [36, 73]

$$R_{ij} - \frac{1}{2}(1 - 2k\lambda)g_{ij}R = kT_{ij}, \quad (2.1)$$

where R_{ij} represents the Ricci tensor, g_{ij} denotes the metric tensor, and T_{ij} stands for the energy-momentum tensor (EMT). The parameter k is the gravitational coupling constant, whose value is fixed by ensuring consistency with the Newtonian limit. The standard Einstein field equations are recovered when $\lambda = 0$ and $k = 8\pi$, under the condition of covariant conservation of the energy-momentum tensor, $T_{;i}^{ij} = 0$.

Hence, the trace involved in Eq. (2.1) can easily be presented in the following form [73]

$$(4k\lambda - 1)R = kT, \quad (2.2)$$

from where one can notice that the energy-momentum tensor becomes traceless (i.e. $T = 0$) when either $R = 0$ or $k\lambda = \frac{1}{4}$. Hence, it is important to highlight that the Rastall theory exhibits behavior analogous to GR in the case of a vanishing Ricci scalar ($R = 0$), while the EMT trace disappears when $k\lambda = \frac{1}{4}$. When $k\lambda \neq \frac{1}{4}$, the gravitational field equations incorporating the cosmological constant Λ can be expressed as follows

$$G_{ij} + \Lambda g_{ij} + k\lambda g_{ij}R = kT_{ij}, \quad (2.3)$$

where G_{ij} represents a typical tensor after the name of Einstein.

The homogeneous and isotropic metric, i.e., the Friedmann–Lemaître–Robertson–Walker (FLRW) line element is adopted here to describe a universe in its usual format

$$ds^2 = -dt^2 + a^2(t) \left(\frac{dr^2}{1 - Kr^2} + r^2 d\Omega^2 \right), \quad (2.4)$$

where $d\Omega^2 = d\theta^2 + \sin^2 \theta d\phi^2$. It is to note that the cosmic expansion is governed by the scale factor $a(t)$, which depends on time, while the spatial curvature index K specifies the geometry of the universe, where $K = -1, 0, +1$ represent open, flat, and closed spatial configurations, respectively.

In the context of a ideal fluid distribution, the field equations in the Rastall theory can be written as [36, 46, 47, 73]

$$(3 - 12\lambda k)H^2 - 6k\lambda \dot{H} + (3 - 6k\lambda) \frac{K}{a^2} = k\rho, \quad (2.5)$$

$$(3 - 12k\lambda)H^2 - (6K\lambda - 2)\dot{H} + (1 - 6\lambda k) \frac{K}{a^2} = -kP, \quad (2.6)$$

where P denotes the cosmic pressure and ρ represents the energy density while the symbol over-dot denotes differentiation under the cosmic time t whereas a is the scale factor which is attached to the Hubble parameter via the relation $H = \dot{a}/a$.

For the considered model, the cosmic fluid pressure and matter-energy density are associated via the barotropic equation of state $P = w\rho$, with symbol w as the EOS parameter. Using the Bianchi identity, expressed as $G_{ij}^{;j} = 0$, one can obtain the energy-momentum conservation (continuity) equation [73]

$$(1 - 3\lambda k)\dot{\rho} - 3\lambda k\dot{P} + (3 - 12\lambda k)(P + \rho)H = 0. \quad (2.7)$$

Most of the cosmological observational data are expressed as function of the redshift z instead of t . Typically the cosmic scale factor $a(t)$ is related to z via the $a_0/a = 1 + z$ relationship with a_0 as the presently considered value of the scale factor (which we have assumed as unity in the present study). By using this relation, the time derivative of the Hubble parameter can be presented in the following form: $\dot{H}(t) = -(1 + z)H(z)H'(z)$, as such $H'(z) = \frac{dH}{dz}$. Consequently, the field equations given in Eqs. (2.5) and (2.6) can be rewritten in terms of the redshift parameter z as follows

$$(3 - 12k\lambda)H^2 + 6k\lambda(1 + z)HH'(z) + K(3 - 6k\lambda k)(1 + z)^2 = k\rho, \quad (2.8)$$

$$(3 - 12k\lambda)H^2 + (1 + z)H(6k\lambda - 2)H'(z) - K(6k\lambda - 1)(1 + z)^2 = -kP. \quad (2.9)$$

To explain DE related cosmological phenomena, various theoretical models have been proposed in literature, however none of them could explain it in a significant and efficient way. To understand the physical dynamics of the universe, therefore we need parameterization. However, a model-independent technique is the well-known alternative for verifying the dynamics of DE models [74]. This strategy aims to follow the parameterization of the any one of the cosmic parameters, i.e., the Hubble parameter, Deceleration Parameter (DP), and EOS parameter, as required for any auxiliary equations. Considering the parameterization of $H(z)$, the state-finder diagnostic has been examined in Ref. [75]. In addition, several parameterizations have been attempted by different authors for exploration of the dynamic attributes of our universe which include CPL (Chevallier-Polarski-Linder), BA (Barboza-Alcaniz), LC (Low Correlation) [76], and the DP [77].

In the literature, therefore the above mentioned parameterizations have been extensively considered for issues with cosmological researches (vide Ref. [78] for a comprehensive overview). Under such motivation, we consider here parameterization of the Hubble parameter $H(z)$ in the logarithm form as [79]

$$H^2(z) = H_0^2 \left[(z + 1)^3 A + B + \eta \log(1 + z) \right], \quad (2.10)$$

with H_0 , A , B , and η as free parameters.

In the above Eq. (2.10), the normalizing feature H_0 confirms that the free parameters A and η are dimensionless and of order unity. This parameterization enables us to analyze the dynamics of a cosmic model beyond the conventional Λ CDM model across both high and low redshift ranges. Later on one can observe that by using the same parametrization as of Ref. [79], a better model is possible to provide based on data analytic approaches which does altogether represent a valid scenario of late time accelerated universe.

From Eq. (2.10), we get the relation $A + B = 1$ at $z = 0$. Within the Λ CDM cosmological framework, the Hubble parameter is expressed as follows

$$H(z) = H_0 \sqrt{\Omega_{m0}(z + 1)^3 + \Omega_\Lambda}. \quad (2.11)$$

Here, H_0 is the current value of Hubble constant whereas Ω_{m0} and Ω_Λ are the current values of density parameters of matter and dark energy. The parameterization Eq. (2.10) can be reduced into the Λ CDM cosmology if $A = \Omega_{m0}$, $B = (1 - \Omega_{m0})$, and $\eta = 0$. However, the addition of the term $\eta \log(1 + z)$ provides a kind of logarithmic modification that is introduced to enhance the model's adaptability in describing more intricate features of the cosmic expansion history. This formulation is motivated by the objective of examining possible departures from the Λ CDM framework, which relies on a constant cosmological term Λ along with a fixed matter density parameter. By incorporating the logarithmic component, an extra adjustable parameter is introduced, allowing the model to capture evolution patterns in the expansion rate that may not be fully represented by simpler parameterizations. This kind of generality is useful to test the model against observational constraints and evaluating its potential to more accurately reflect the actual expansion dynamics of the universe [80, 81].

For the considered model, the DP can be written as

$$q = H^{-2} \dot{H} - 1. \quad (2.12)$$

III. METHODOLOGIES AND DATASETS

In this section, we perform data analysis under statistical as well as ML based discussion.

A. Statistical analysis

A-1: Statistical analysis by using the primary observational datasets

Bayesian inference has emerged as a cornerstone methodology in contemporary cosmological research for parameter estimation and model comparison. In this investigation, we aim to determine constraints on the free parameters of our cosmological framework by analyzing various observational datasets through a χ^2 -minimization approach. To derive estimates for the model parameters A , B , η , and H_0 , we utilize the following observational datasets:

(i) **Cosmic Chronometers (CC):** The cosmic chronometer technique offers direct observational measurements of the Hubble parameter $H(z)$ derived from the differential age evolution analysis of galaxies. Our analysis incorporates a compilation comprising 31 observational data points distributed across the redshift range $[0.07, 1.965]$ [82, 83].

(ii) **Pantheon sample:** Here we employ the most latest sample of SNIa within the redshift interval $[0.001, 2.26]$ [84]. It is to be noted that this dataset integrates observations from around 18 distinct surveys which include all light curves normalized by using the SALT2 fitting procedure and thus to maintain consistent calibration throughout the dataset [85].

(iii) **Baryon Acoustic Oscillation (BAO) Data:** Our analysis incorporates six BAO measurements derived from various galaxy surveys, such as SDSS DR7, 6dF, and WiggleZ [86–88]. Here the angular diameter distance can be provided in the following form

$$d_A = \frac{D_L}{(1+z)^2}, \quad (3.1)$$

where D_L denotes the luminosity distance [89].

Again, the scale of dilation is formulated as

$$D_V(z) = \left[\frac{cz(D_L(z))^2}{(1+z)^2 H(z)} \right], \quad (3.2)$$

$$D_V(z) = \left[D_L^2(z)(1+z)^{-2} \frac{cz}{H(z)} \right]^{1/3}. \quad (3.3)$$

For constraining the model parameters, we define the chi-square estimator for the BAO observations as [89–92]

$$\chi_{\text{BAO}}^2 = X^T C^{-1} X, \quad (3.4)$$

where C represents the covariance matrix and the vector X is given by

$$X = \begin{pmatrix} \frac{d_A(z_*)}{D_V(0.106)} - 30.95 \\ \frac{d_A(z_*)}{D_V(0.20)} - 17.55 \\ \frac{d_A(z_*)}{D_V(0.35)} - 10.11 \\ \frac{d_A(z_*)}{D_V(0.44)} - 8.44 \\ \frac{d_A(z_*)}{D_V(0.60)} - 6.69 \\ \frac{d_A(z_*)}{D_V(0.73)} - 5.45 \end{pmatrix}. \quad (3.6)$$

One can evaluate the parametric values of the model, such as A , B , η , and H_0 , through the observational evidences and statistical techniques. Here, E_{obs} denotes the measured value from observational data, whereas E_{th} signifies the theoretically predicted values within our cosmological framework. Through statistical

Table I. Datasets of z_{BAO} and $\varphi(z)$ to evaluate $\Upsilon(z)$. Here, we exploit the relationship $\varphi(z) = d_A(z_*)/D_V(z_{\text{BAO}})$ with $z_* \approx 1091$ [89]).

z_{BAO}	0.106	0.2	0.35	0.44	0.6	0.73
$\varphi(z)$	30.95 ± 1.46	17.55 ± 0.60	10.11 ± 0.37	8.44 ± 0.67	6.69 ± 0.33	5.45 ± 0.31

comparison of E_{obs} and E_{th} , we can determine the optimal parameter values. For achieving the most precisely obtained values, we execute the χ^2 estimator as follows

$$\chi^2 = \sum_{i=1}^N \left[\frac{E_{\text{th}}(z_i) - E_{\text{obs}}(z_i)}{\sigma_i} \right]^2, \quad (3.7)$$

where $E_{\text{th}}(z_i)$ presents the theoretical parametric values, $E_{\text{obs}}(z_i)$ denotes the measured values, σ_i indicates the associated uncertainty (i.e., the standard error), where N stands for the total points of data employed in the sample.

The combined χ^2 estimator can be given by

$$\chi^2_{\text{combined}} = \chi^2_{\text{CC}} + \chi^2_{\text{Pantheon}} + \chi^2_{\text{BAO}}. \quad (3.8)$$

In the context of the χ^2_{tot} statistics, a few technical points are as follows that one can make it minimized in order to get the parametric value which could be best fitted to the datasets of the joint sample of CC, Pantheon, and BAO. Therefore, (i) under the approach of the maximum likelihood, $\mathcal{L}_{\text{tot}} = \exp(-\chi^2_{\text{tot}}/2)$, known as the total likelihood function and can be expressed as: $\mathcal{L}_{\text{tot}} = \mathcal{L}_{\text{BAO}} * \mathcal{L}_{\text{Pantheon}} * \mathcal{L}_{\text{CC}}$; (ii) either the likelihood function $\mathcal{L}_{\text{tot}}(x^*)$ can be considered as maximized or $\chi^2_{\text{tot}}(x^*) = -2 \ln \mathcal{L}_{\text{tot}}(x^*)$ can be assumed as minimized so that the most plausible values of parameters can be obtained; (iii) within the setting of the constraints (such as x^* , 1σ and 2σ), we observe that parameters are fitted and also restricted for $\chi^2_{\text{tot}}(x) = \chi^2_{\text{tot}}(x^*) + 2.3$ and $\chi^2_{\text{tot}}(x) = \chi^2_{\text{tot}}(x^*) + 6.17$; (iv) one can get the best-fit parametric values by minimizing the χ^2 statistics (see Table I along with the illustrated Fig. 1).

A-2 : Statistical analysis with the latest datasets (CMB, BAO-DESI and Union 3.0)

Here, we conduct analysis with the latest datasets of CMB, BAO-DESI, and Union 3.0 in addition with CC dataset [93–100] which can be seen in Fig. 2 (also inquisitive readers may be interested in Table II for a few collected numerical values on the Hubble parameter derived from CC and BAO methodology).

(i) Union 3.0: In the present analysis, the Union 3.0 latest dataset derived from the recent SN Ia. This is a largest dataset compiled from 24 different samples of Type Ia supernovae by an unified Bayesian process and consists of 2087 SNIa within the redshift range $0.01 < z < 2.26$ [93]. It is to clarify here that in the present analysis, we employ available binned dataset which is based on the distance moduli for this sample. It to be noted that the provided dataset is based on the observation of apparent magnitude (m). However, the distance modulus can then be given by

$$\mu(z) = m_{\text{B}}(z) - M_{\text{B}} = 5 \log_{10} \left(\frac{d_{\text{L}}(z)}{\text{Mpc}} \right) + 25, \quad (3.9)$$

with d_{L} as the luminosity distance which can be provided as

$$d_{\text{L}}(z) = c(1+z) \int_0^z \frac{dz'}{H(z')}. \quad (3.10)$$

However, there are argument that the luminosity (or absolute magnitude) of SN Ia may not evolve with the cosmic redshift [94] and therefore, the SN Ia sample is observed to distributed over a mean absolute magnitude for which $MB = -19.22$ [95].

(ii) CMB: In the present investigation, we employ the CMB distance priors as available in the following work [96] which have been obtained from the Planck 2018 temperature and polarization data (i.e., TT, TE,

Table II. The present value of the Hubble parameter. Here, M_1 and M_2 are the representatives of CC and BAO methods, respectively.

z	H_0 (km s $^{-1}$ Mpc $^{-1}$)	Method	Reference
0.07	69 ± 19.6	M_1	[122]
0.09	69 ± 12	M_1	[123]
0.12	68.6 ± 26.2	M_1	[122]
0.17	83 ± 8	M_1	[123]
0.1791	75 ± 4	M_1	[124]
0.1993	75 ± 5	M_1	[124]
0.2	72.9 ± 29.6	M_1	[122]
0.27	77 ± 14	M_1	[123]
0.28	88.8 ± 36.6	M_1	[122]
0.352	83 ± 14	M_1	[124]
0.38	81.9 ± 1.9	M_2	[125]
0.3802	83 ± 13.5	M_1	[126]
0.4	95 ± 17	M_1	[123]
0.4004	77 ± 10.2	M_1	[126]
0.4247	87.1 ± 11.2	M_1	[126]
0.44497	92.8 ± 12.9	M_1	[126]
0.4783	80.9 ± 9	M_1	[126]
0.48	97 ± 62	M_1	[127]
0.593	104 ± 13	M_1	[126]
0.68	92 ± 8	M_1	[126]
0.781	105 ± 12	M_1	[126]
0.875	125 ± 17	M_1	[126]
0.88	90 ± 40	M_1	[127]
0.9	117 ± 23	M_1	[123]
1.037	154 ± 20	M_1	[126]
1.3	168 ± 17	M_1	[123]
1.363	160 ± 33.6	M_1	[128]
1.43	177 ± 18	M_1	[123]
1.53	140 ± 14	M_1	[123]
1.75	202 ± 40	M_1	[123]
1.965	186.5 ± 50.4	M_1	[128]

and EE + lowE) [97]. Essentially, these priors encode a few crucial geometric information from the entire spectrum of CMB which is accompanied with the shift parameter (i.e., R_{shift}), the acoustic scale (i.e., l_A), and the baryon density (i.e., $\Omega_b h^2$). All of them permit us to incorporate CMB constraints and the fact is that one can do this operation even without estimating the entire set of perturbative procedures.

Therefore, one can incorporate all the aforesaid parameters within the CMB distance prior dataset, i.e., R_{shift} , l_A , and $\Omega_b h^2$ which can be evaluated as

$$l_A = (1 + z_*) \frac{\pi D_A(z_*)}{r_s(z_*)}, \quad R_{\text{shift}} = \frac{(1 + z_*) D_A(z_*) \sqrt{\Omega_m H_0^2}}{c}, \quad (3.11)$$

where z_* and $r_s(z_*)$ are, respectively, the redshift at the decoupled epoch of photon and the co-moving sound horizon at the defined epoch.

(iii) BAO-DESI: For the analysis, we use the BAO-DESI data consists of 12 BAO samples obtained from observations on various tracers of the Dark Energy Spectroscopic Instrument (DESI) [98–100]. The observable measurements in this dataset are $d_M(z)/r_d$, $d_H(z)/r_d$, and $d_V(z)/r_d$, where $d_M(z) = d_L(z)/(1 + z)$,

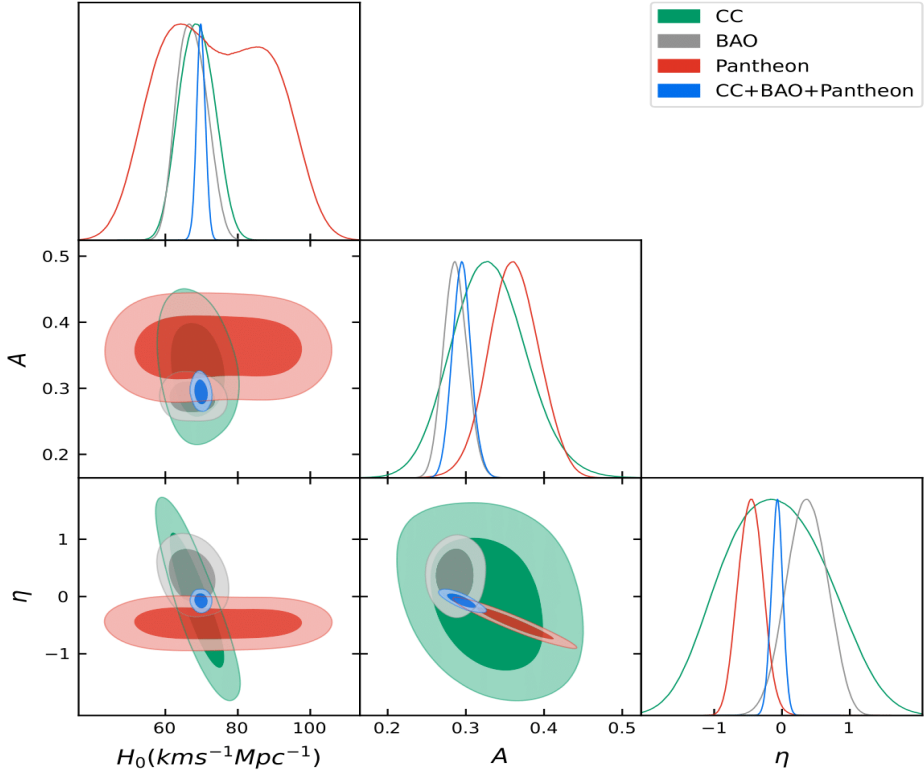


Figure 1. Contour based on the model parameters with 1σ and 2σ confidence levels for CC, Pantheon, BAO, and joint datasets.

$d_{\text{H}}(z) = c/H(z)$, $d_{\text{V}}(z) = [zd_{\text{H}}(z)d_{\text{M}}^2(z)]^{1/3}$, and r_{d} are, respectively, the co-moving distance (transverse type), the Hubble distance, the spherically angular diameter (averaged distance) and the sound horizon scale at the baryon drag epoch as a cosmological standard ruler.

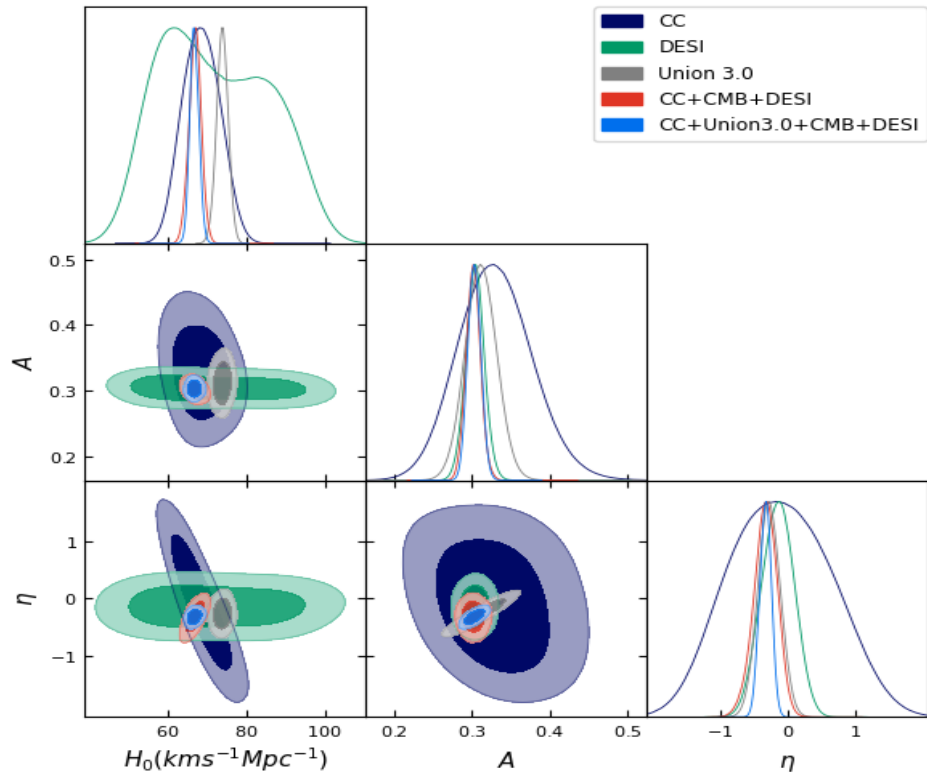


Figure 2. Contour based on the model parameters with 1σ and 2σ confidence levels for CC, Union 3.0, CMB, DESI, and joint datasets.

B. Machine Learning technique

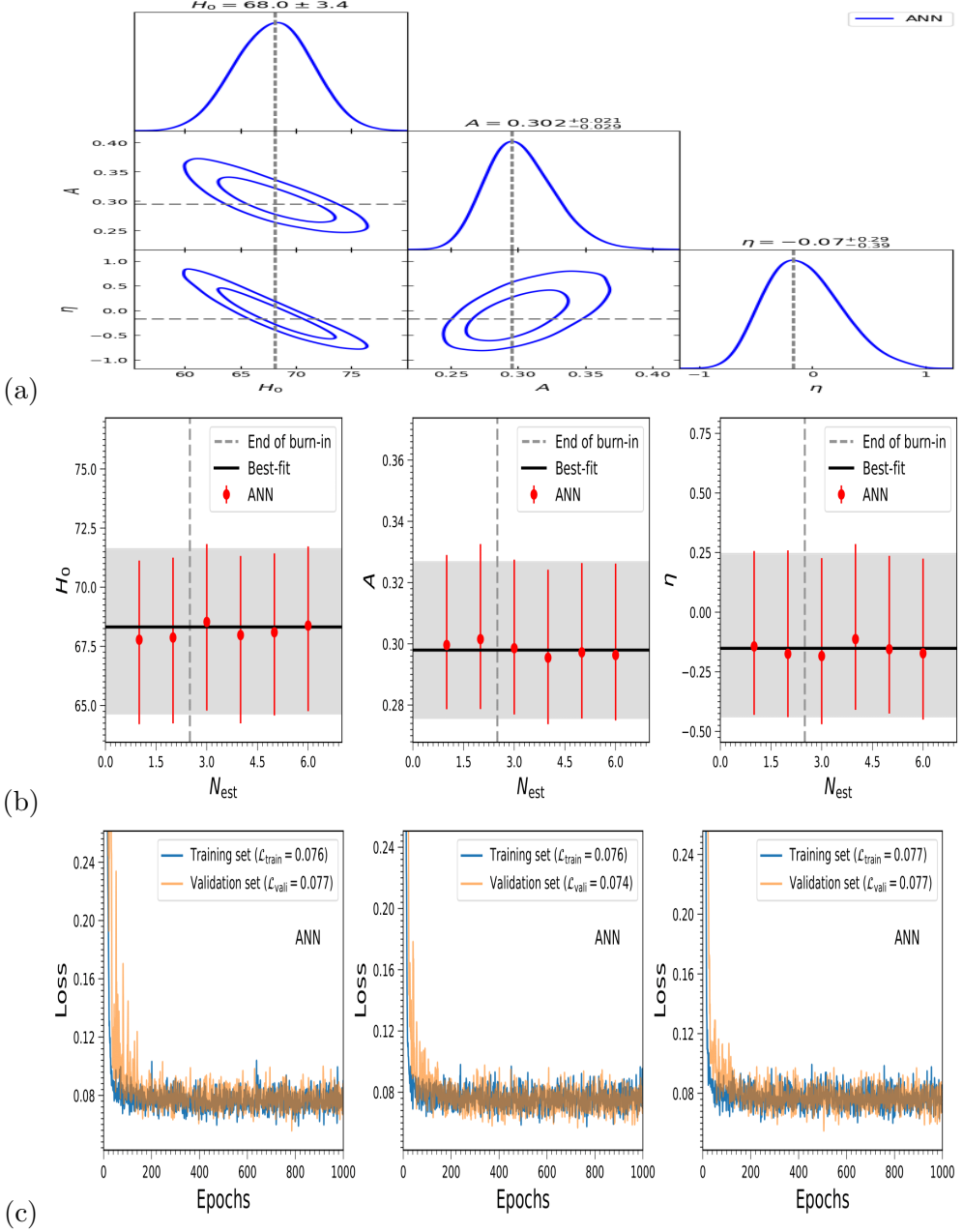


Figure 3. Observational investigation of the Rastall theory based cosmology under ANN model: (a) contours drawn from $H(z)$ data for A , η , and H_0 1σ and 2σ , (b) relationship in between steps as well as best-fit values within 1σ error of model parameters (where the solid black line and Grey-shaded parts display the best-fit values, while the red circle with error bars), and (c) graphical presentation of losses regarding the training and validation sets. Here, the training set consists of 2000 samples whereas the validating set contains 500 samples.

Nowadays, it is noted that due to the advancement in computing, neural network is gradually becoming a very effective and relevant tool leading to the emergence of a novel data analytic arena known as Deep Learning (DL), which acts as a subset of ML (already mentioned earlier) that uses multi-layered artificial neural networks. In the present investigation, we are thinking to apply the deep neural network in its fundamental aspect which is normally known as the multilayer perceptron (MLP). However, we have treated the performances in the following two steps; (i) analysis with the primary datasets, and (ii) analysis with the latest datasets for CMB, BAO, DESI and Union 3.0. Apparently, the behavior and looking are

too similar to distinguish each figures on ANN, MDN, and MNN for the primary as well as the latest datasets. Therefore, we put all the figures based on primary datasets in the following relevant places (as being important figures) and all figures on latest datasets are placed in Appendix (see Figs. 9–11) to get a comparative flavor of the obtained results via graphical presentations.

B-1: Analysis with the primary datasets

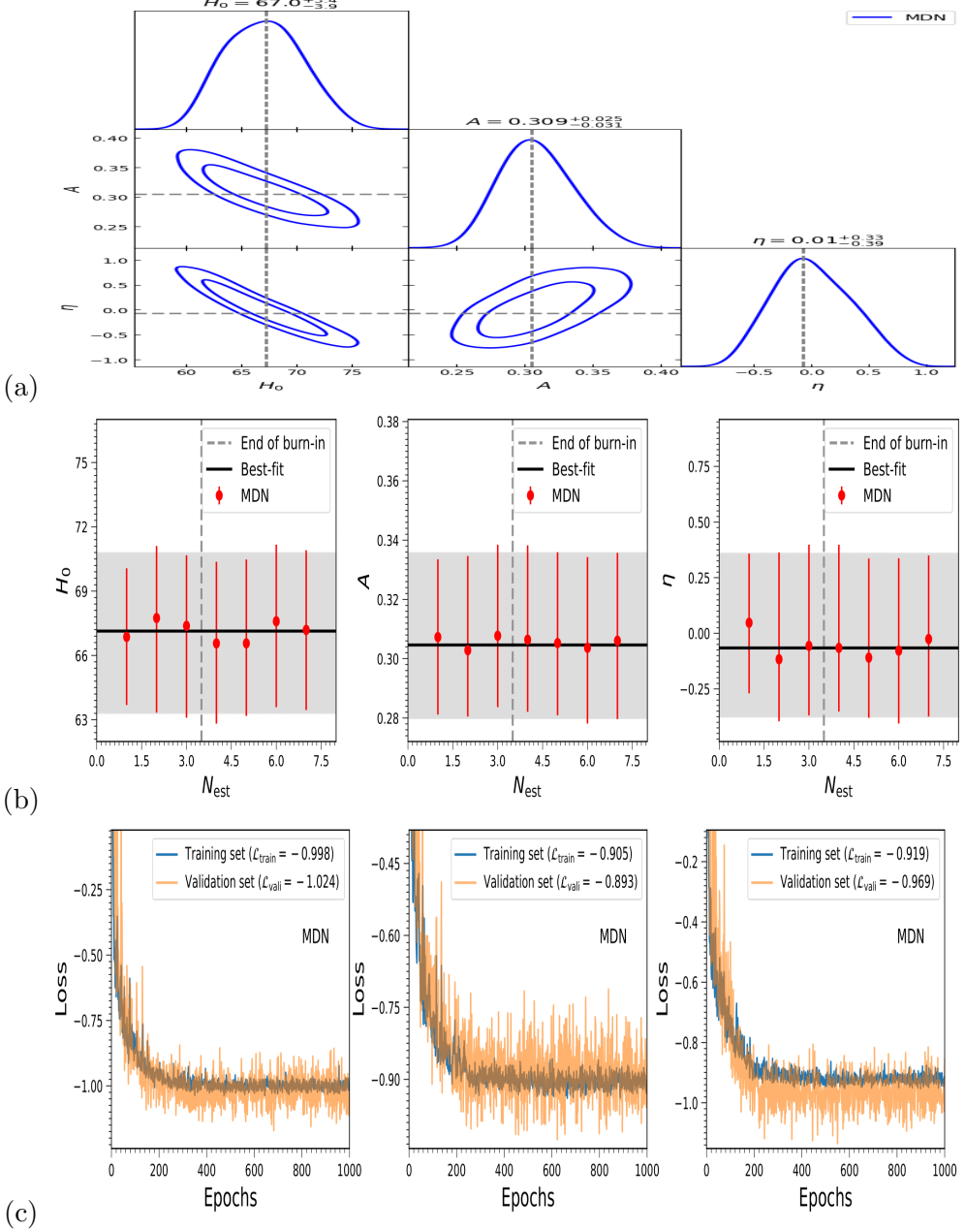


Figure 4. Cosmological quantities in the Rastall theory under MDN model. The legends of (a), (b), and (c) are the same as Fig. 3.

(i) Artificial Neural Network (ANN): This is, in general, referred to as *Neural Network* (NN) which essentially provides a estimating platform to act as a modeling tool. Here, the procedure is as follows: an input layer, may be one or sometimes multiple hidden layers as require due to the demand of the priority or situation, and obviously an output layer. In the case of explicit applications to the cosmological parametric estimation, the generalized methodology is therefore: observational measurements enter through the input layer and are processed through the hidden layers, and thereby eventually producing parametric values of

the concerned cosmological model at the expected output layer of the corresponding exit point of the system. Here the procedure involves in each layer operation on a vector containing elements (i.e., neurons) and all these stepwise accept inputs from the previous layer of operation. The computational procedure involves in executing a linear transformation which is coupled with a nonlinear activation function. This normally results with the computed output which is subsequently transmitted to the following layer. Generally, no definitive theoretical guideline exists for selecting the ideal number of neurons to incorporate within each hidden layer. In our investigation, we implement the network design suggested in Ref. [61], where the neuron count in consecutive hidden layers diminishes progressively as the layer depth increases, facilitating effective feature extraction while minimizing computational demands.

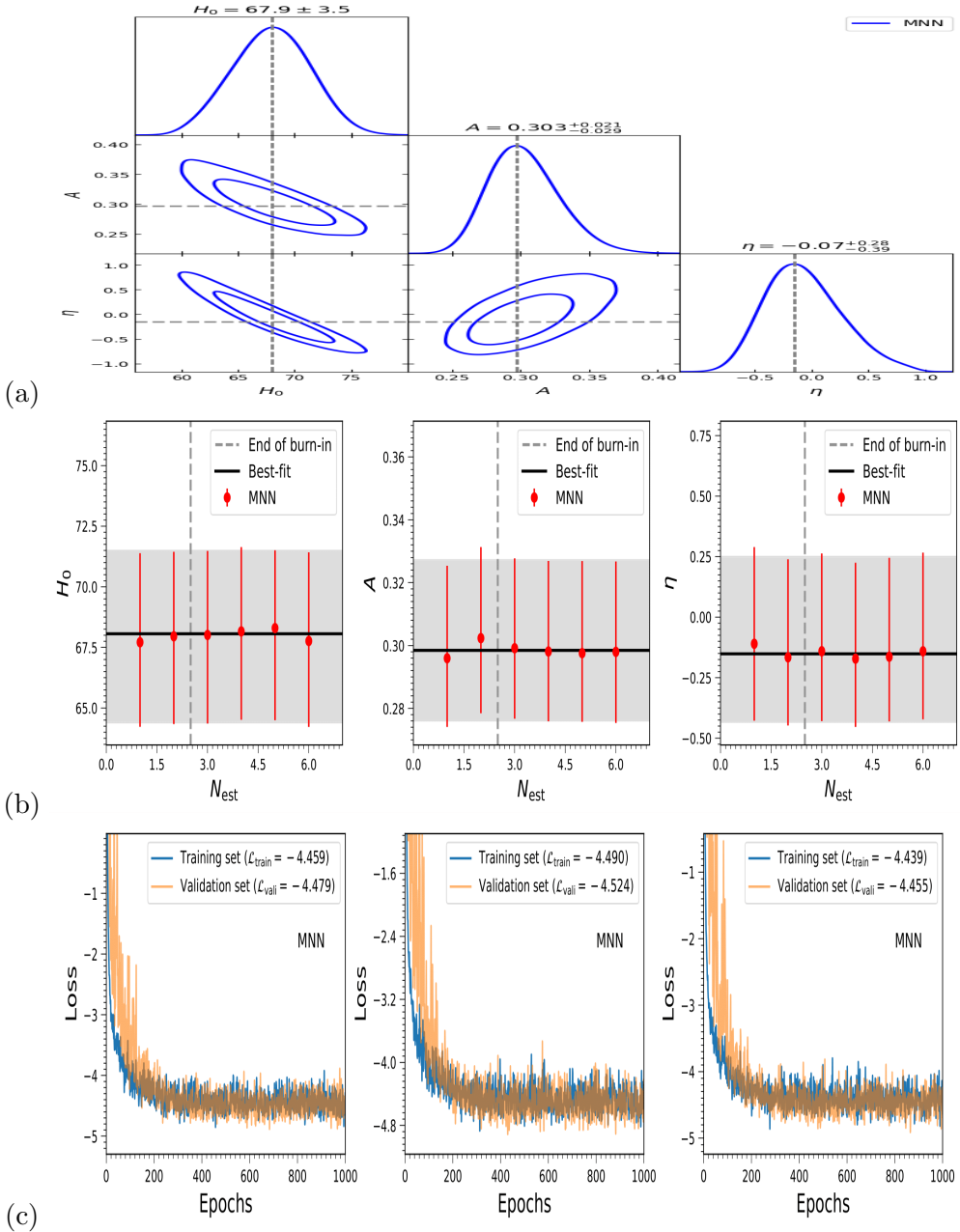


Figure 5. Cosmological quantities in the Rastall theory under MNN model. The legends of (a), (b), and (c) are the same as Fig. 3.

(ii) Mixture Density Network (MDN) This technique properly and effectively integrates an ANN under a mixture modeling framework. This particular mixture modeling technique provides a probabilistic approach on the basic assumption that each data point evolves from a weighted merging for a finite set

of probability distributions with unspecified parametric values. Interestingly, these distributions may often belong to different types of probability families which includes Gaussian or beta type distribution. The basic objective of this parametric estimation by using the MDN is to evaluate different unknown parameters which essentially refer to a combined model [61]. Hence, an MDN performing Gaussian fraction properly establishes a mapping among the observationally measured datasets and the model parameters which characterizes Gaussian mixture so that the parameters can be optimized through a technique of minimization of the loss function.

(iii) Mixture Neural Network (MNN)

The Mixture Neural Network (MNN) technique is a posterior distribution that can be exhibited as a merging of various unknown component distributions. The MNN considers this mixture model via an ANN. Here, in this methodology, the steps are as follows: firstly, estimation of the parameters, secondly, by producing samples from the learned mixture reformatting of the posterior distribution is performed. However, in the case of various cosmological parameters whose distributions deviate from the Gaussian feature, essentially multiple mixture components are required to precisely approximate the posterior [61]. This obviously increases the computational hazard, as training the network becomes more time-consuming and potentially unstable and hence making the learning of mixture parameters much more challenging.

IV. EXAMINATION OF THE MODEL'S COSMOLOGICAL FEATURES

In this section, we perform several testings of our model to explore different cosmological attributes with graphical illustrations.

A. EOS parameter

We have the cosmic density and fluid pressure in the following forms

$$\begin{aligned} \rho = 3 & \left[(1 - 4\lambda)H_0^2 ((z + 1)^3 A + B + \eta \log(z + 1)) \right. \\ & \left. + \lambda (3(z + 1)^3 A + \eta) H_0^2 + k(1 - 2\lambda)(z + 1)^2 \right], \end{aligned} \quad (4.1)$$

$$\begin{aligned} P = -3(1 - 4\lambda)H_0^2 & ((z + 1)^3 A + B + \eta \log(z + 1)) \\ & + (1 - 3\lambda) (3(z + 1)^3 A + \eta) H_0^2 - k(1 - 6\lambda)(z + 1)^2. \end{aligned} \quad (4.2)$$

We can note that the Rastall theory based model provides the energy density as positive throughout the evolution of the universe. However, the cosmic pressure initially being positive exhibits a matter-dominated cosmic era. Therefore, for the constraint $w > 0$, the EOS parameter features a Big Bang scenario whereas under $w = 0$ (representing a non-relativistic matter), a matter-dominated universe can be observed. In this case, the constraint $w = 1/3$ (for a relativistic matter) represents a radiation era. Other possibilities are as follows: (i) the model belongs to the quintessence era for the constraint ' $-1 < w \leq 0$ ', (ii) the EOS parameter provides the Λ CDM model for $w = -1$, and (iii) one can observe a phantom scenario for $w < -1$. We have shown the features of w in the left panel of Fig. 6 for the presented model under different EOS conditions. Interestingly, this figure exhibits that the model starts from a Big Bang era and then crossing the quintessence phase approaches to the Λ CDM model universe.

B. Deceleration Parameter (DP)

The DP can suitably be expressed as

$$q = -1 + \frac{(1 + z)}{H(z)} \frac{dH(z)}{dz},$$

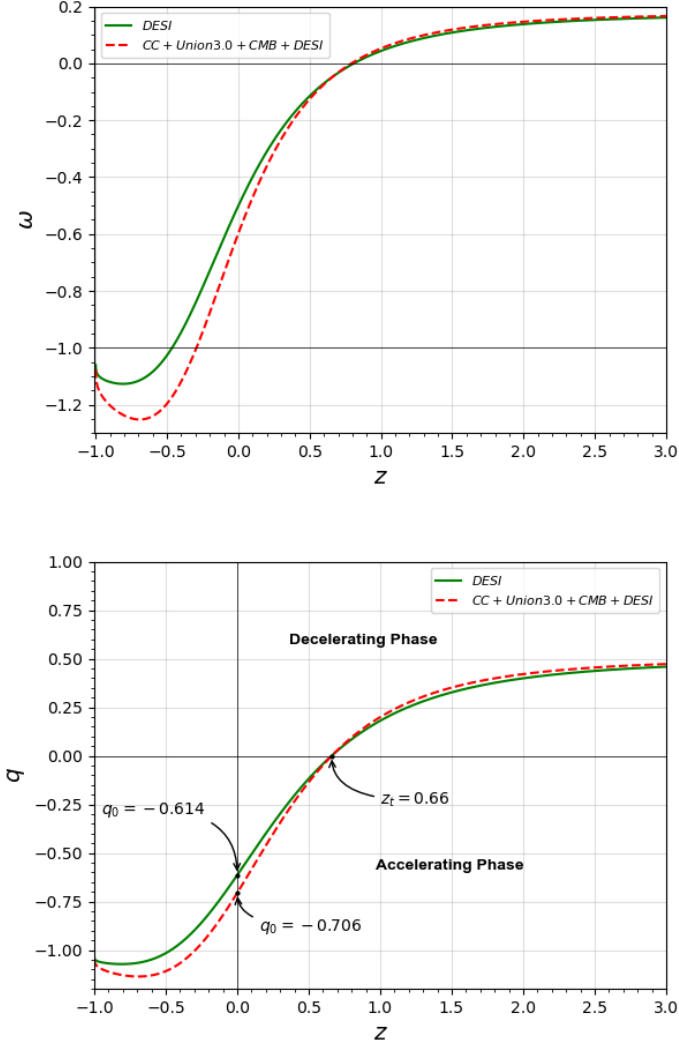


Figure 6. w as a function of z (upper panel) and q as a function of z (lower panel). The solid line (green) shows DESI, and the dotted line (red) depicts CC + Union 3.0 + CMB + DESI datasets.

so that for the undertaken model, it takes the following form

$$q = \frac{A(1+z)^3 - 2B + \eta - 2\eta \log(1+z)}{2[A(1+z)^3 + B + \eta \log(1+z)]}. \quad (4.3)$$

Under this situation, the model exhibits a clear transition of the universe from a decelerating phase in the past to the current accelerating epoch, signifying the dominance of DE at late times and matter domination in the early universe. For the combined datasets of CC, BAO, and Pantheon, the present value of the deceleration parameter is obtained as $q_0 = -0.595$, with the transition (signature flipping) occurring at a redshift $z_t = 0.685$, as illustrated in Fig. 6 (right panel). The results further indicate that as $z \rightarrow -1$, q asymptotically approaches -1 , representing a de Sitter-like future. These findings show strong consistency with recent observational analyses [81–83, 101–104].

C. Statefinders diagnostic

The statefinder parameters (i.e., r and s), can now be introduced for understanding of various DE-based cosmological scenario [105–107] via the evolutionary trajectory on the $r - s$ plane, in special connection to

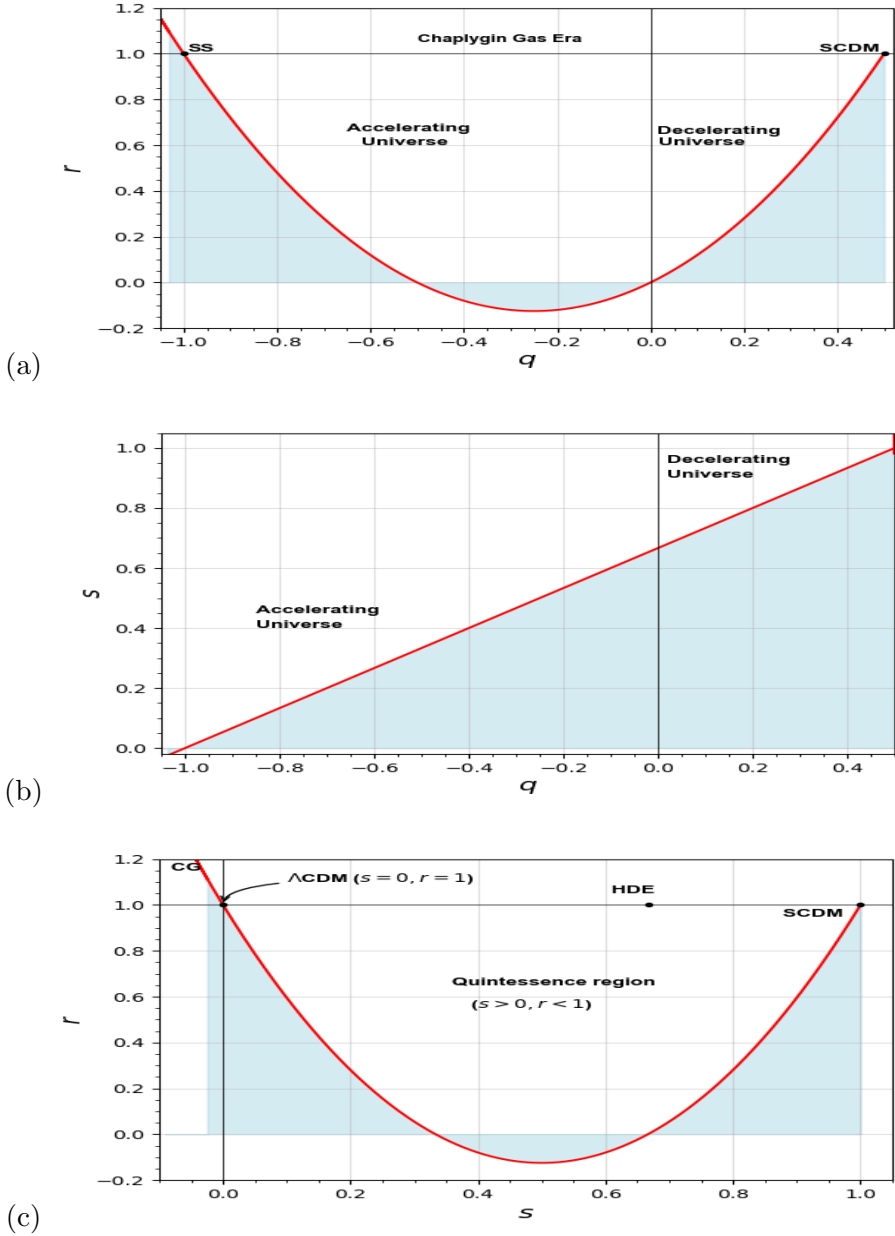


Figure 7. Statefinders diagnostic features: (a) r vs q , (b) s vs q , and (c) r vs s for joint data set of CC, Union 3.0, CMB, and BAO-DESI datasets.

the ΛCDM model [75, 105]. Let us first define r and s as their usual forms, given by

$$r = 2q^2 + q - \frac{\dot{q}}{H}, \quad (4.4)$$

$$s = \frac{r - 1}{3(q - \frac{1}{2})}, \quad (4.5)$$

whereas one can find the explicit forms under the Rastall theory theory in Appendix B.

Figure 7 exhibits the attributes of the present model under the consideration of ‘Chaplygin gas ($r > 1, s < 0$)’ which does converge to the ‘ ΛCDM scenario ($r = 1, s = 0$)’ at the accelerating phases of the cosmos. Under CC, BAO, and Pantheon based joint dataset, (r, s) can be estimated to be $(0.114, 0.270)$ which, therefore, displays features resembling the ΛCDM scenario [75, 106–108].

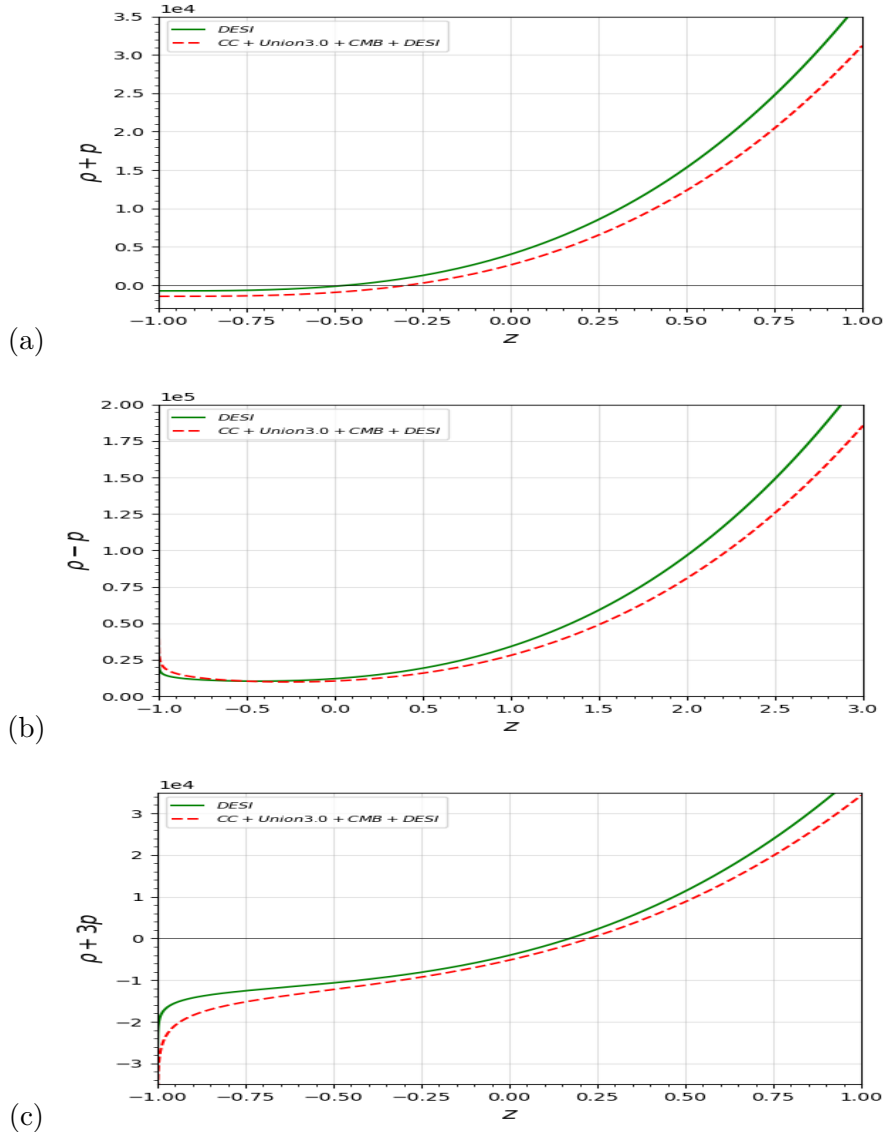


Figure 8. Cosmological evolution of energy conditions in the Rastall theory as a function of the redshift z with a combined datasets (CC, BAO and Pantheon): (a)NEC, (b)DEC, (c)SEC.

V. ENERGY CONDITIONS

The physical viability of the presented model can be verified through the evolution of energy conditions (ECs) [109, 110]. In case of the Rastall theory, the energy conditions can be defined [109–111] as follows: (i) Weak energy conditions (WEC), i.e., $\rho \geq 0$, (ii) Dominant energy conditions (DEC), i.e., $\rho - p \geq 0$, (iii) Null energy conditions (NEC), i.e., $\rho + p \geq 0$, and (iv) Strong energy conditions (SEC), i.e., $\rho + 3p \geq 0$.

It is to noted that, in general, WEC and DEC are quite satisfiable for all the recognized forms of matters and energies [112–114]. However, exotic DE characterized by negative pressure and hence repulsive gravity, is taking the role for the cosmic expansion and SEC violate in the case of DE dominance [112–115].

Figure 8 demonstrate the feature of various energy conditions in the Rastall theory under a combined dataset of CC, BAO, and Pantheon. In this analysis, DEC is satisfied while NEC and Strong Energy Condition (SEC) violates for the proposed model as depicted in Fig. 8 that validates an accelerated expansion of cosmos in the present era [112–116].

In Tables III and IV, one can notice from the numerical values of the parameters that overall both the Tables are complying with the observational findings within the valid ranges. However, in a close view of the datasets indicate some minor changes which can be seen in values of model parameters. The

Table III. Estimated values of the cosmological parameters for the present model by using primary datasets.

Datasets	H_0 (km s $^{-1}$ Mpc $^{-1}$)	A	B	η
CC	68.717 ± 4.955	0.3295 ± 0.0459	0.6705 ± 0.0459	-0.1011 ± 0.7929
BAO	$67.434^{+3.912}_{-4.401}$	0.2858 ± 0.0137	0.7142 ± 0.0137	0.3710 ± 0.2920
Pantheon	74.178 ± 17.093	0.3614 ± 0.0292	0.6386 ± 0.0292	-0.4631 ± 0.1786
CC+BAO+Pantheon	69.835 ± 1.162	0.2946 ± 0.0124	0.7054 ± 0.0124	-0.0744 ± 0.0881
ANN	68.00 ± 3.40	$0.302^{+0.021}_{-0.029}$	$0.698^{+0.021}_{-0.029}$	$-0.070^{+0.290}_{-0.390}$
MDN	$67.00^{+3.40}_{-3.90}$	$0.309^{+0.025}_{-0.031}$	$0.691^{+0.025}_{-0.031}$	$0.010^{+0.330}_{-0.390}$
MNN	67.90 ± 3.50	$0.303^{+0.021}_{-0.029}$	$0.697^{+0.021}_{-0.029}$	$-0.070^{+0.280}_{-0.390}$

Table IV. Estimated values of the cosmological parameters for the present model by using the latest observational datasets.

Datasets	H_0 (km s $^{-1}$ Mpc $^{-1}$)	A	B	η
CC	68.717 ± 4.955	0.330 ± 0.046	0.6705 ± 0.046	-0.101 ± 0.793
DESI	72.141 ± 15.533	0.3042 ± 0.0119	0.696 ± 0.0119	-0.141 ± 0.257
Union 3.0	74.047 ± 1.373	0.312 ± 0.019	0.688 ± 0.019	-0.269 ± 0.154
CC+CMB+DESI	67.125 ± 1.430	0.302 ± 0.009	0.698 ± 0.009	-0.321 ± 0.158
CC+CMB+DESI+Union 3.0	66.945 ± 1.094	0.304 ± 0.008	0.696 ± 0.008	-0.322 ± 0.0895
ANN	67.00 ± 0.470	0.301 ± 0.024	0.699 ± 0.024	-0.300 ± 0.190
MDN	67.040 ± 0.490	0.302 ± 0.025	0.698 ± 0.025	-0.320 ± 0.210
MNN	67.010 ± 0.470	0.301 ± 0.024	0.699 ± 0.024	-0.300 ± 0.190

latest dataset of DESI-BAO, when clubbed with CC, CMB, and Union 3.0 determine the Hubble tension $H_0 = 66.945 \pm 1.094$ which suitably aligned with the findings from the observational evidences reported by Li et al. [117].

VI. CONCLUSIONS

The present manuscript examines a transitioning cosmological framework implemented through the Rastall theory. We have constructed the relevant field equations within a homogeneous and isotropic spacetime geometry under this theory. To find analytical solutions, we have used a logarithmic representation of the Hubble parameter (see Eq. (10)). Constraints on the model parameters were determined by analyzing observational evidence from different datasets, e.g., BAO, Pantheon, and CC, by using standard MCMC methodology.

To enhance the precision of cosmological parameter estimation and investigation of the current cosmic acceleration phase, we have incorporated an advanced DL technique. By implementing the CoLFI Python package combined with neural architectures including Artificial Neural Networks (ANN), Mixture Density Networks (MDN), and Mixture Neural Networks (MNN), alongside contemporary cosmological observations (CMB, BAO, DESI, and Union 3.0), we achieved efficient parameter determination. This methodology significantly has enhanced our comprehension of the provisional likelihood functions obtained from observational evidence and their associated posterior probability distributions (illustrated in Figs. 3–5 as well as in Figs. 9–11).

Under this motivation we have performed statefinder diagnostic evaluation which reveals that our model demonstrates behavior analogous to the Λ CDM paradigm during the current epoch, while exhibiting certain deviations from complete conformity (illustrated in Fig. 7). We note that there is a violation of SEC in the Rastall theory framework which therefore provides evidence in support of the accelerated expansion phase of the universe in contemporary times (illustrated in Fig. 8). Therefore, our examination of fundamental cosmic quantities – which include the pressure, energy density, EOS parameter, and DP – reveals that the

Table V. Comparison of the current value of the Hubble parameter: the present model vs other models in the literature.

Datasets	H_0 (km s $^{-1}$ Mpc $^{-1}$)			
DESI	72.141 ± 15.533 ^a	73.43 ± 2.97 [118]	$68.4_{-0.8}^{+1.0}$ [119]	68.53 ± 0.80 [98]
Union 3.0	74.047 ± 1.373 ^b	$73.38_{-2.82}^{+3.12}$ [118]	$74.912_{-1.805}^{+2.015}$ [120]	67.93 ± 0.42 [121]

^a Data derived from the present model

^b Data derived from the present model

presented model produces physically meaningful and consistent outcomes (illustrated in Figs. 6–8).

Furthermore, employment of the hyper-ellipsoid constraints contributed to enhance stability during neural network optimization as well as improved the accuracy of the concerned parameter determination. A comparative evaluation among the modern NN-based approaches and that of the traditional MCMC methodology revealed that the MNN technique produced results in close agreement with MCMC outcomes, thus confirming its effectiveness and dependability for cosmological parameter inference.

Our cosmological model successfully accounts for the late-time cosmic acceleration without invoking any mysterious DE, thereby circumventing complications related to the erstwhile cosmological constant. This emphasizes the significance of incorporating current observational constraints when modeling within the Rastall theory paradigm. Our results demonstrate that neural network approaches provide an effective methodology for determining cosmological parameters, offering a practical complement to MCMC methodologies. The Rastall theory paradigm enables investigations of diverse gravitational astrophysics and their influence on cosmic expansion dynamics utilizing ANN, MNN, and MDN frameworks. Evidently, this investigation forms part of an extensive program merging cosmology with ML, showcasing ML-based technical capability for addressing complex cosmic dynamics and expansion phenomena (illustrated in Figs. 3–5 and Figs. 9–11).

In Table II, we have shown the Hubble parametric values based on CC and BAO methodology. Tables III (derived values of the parameters for the presented model by using primary datasets) and IV (derived values of the parameters for the presented model by latest observational datasets) present the quantitative values of model parameters. While both tables demonstrate reasonable agreement with observations, however derived from the most recent observational data exhibits superior consistency with observational signatures overall. We have done a bit comparative study in Table V by showing the numerical data of H_0 : our case of the presented model vs a few available data from the literature. A close observation on this Table V shows an overall confirmity and validity of our model in comparison to others investigations.

Essentially, from our investigations by using ML techniques (Tables III and IV), we observe that the Hubble tension for the present model is nearly identical to the estimated value by MCMC for the combined dataset (i.e. CMB, CC, Union 3.0, and DESI-BAO). So, we note that ML approaches (i.e. ANN, MDN, and MNN) work in a better way to get statistical measure of the model parameters.

In summary, the current study has analyzed the Hubble parameter together with the latest DESI-BAO data and DE Survey observations through statistical analysis (particularly the MCMC method) as a primary platform and ML methodology as higher level application. In our future research program, we intend to analyze gravitational wave data utilizing machine learning approaches, which have demonstrated superior performance relative to traditional MCMC methods and may therefore reveal novel physical insights and open new research directions within our adopted framework.

ACKNOWLEDGMENTS

SR sincerely acknowledges the support of the Inter-University Centre for Astronomy and Astrophysics (IUCAA), Pune, India, through its Visiting Research Associateship Programme, during which part of this study was carried out. The research work of KB was partially supported by the JSPS KAKENHI

Grant Numbers 24KF0100, 25KF0176 and the Competitive Research Funds for the Faculty of Fukushima University (Grant No. 25RK011).

APPENDIX A

In this appendix, we apply the ML technique to estimate the model parameters by utilizing the latest datasets of CMB, BAO-DESI, Union 3.0 etc. However, the discussion for the primary datasets with graphical presentations are exhibited in section III (B-1) with Figs. 3–5. Below the Figs. 9–11 exhibit features for (i) ANN, (ii) MDN, and (iii) MNN, respectively.

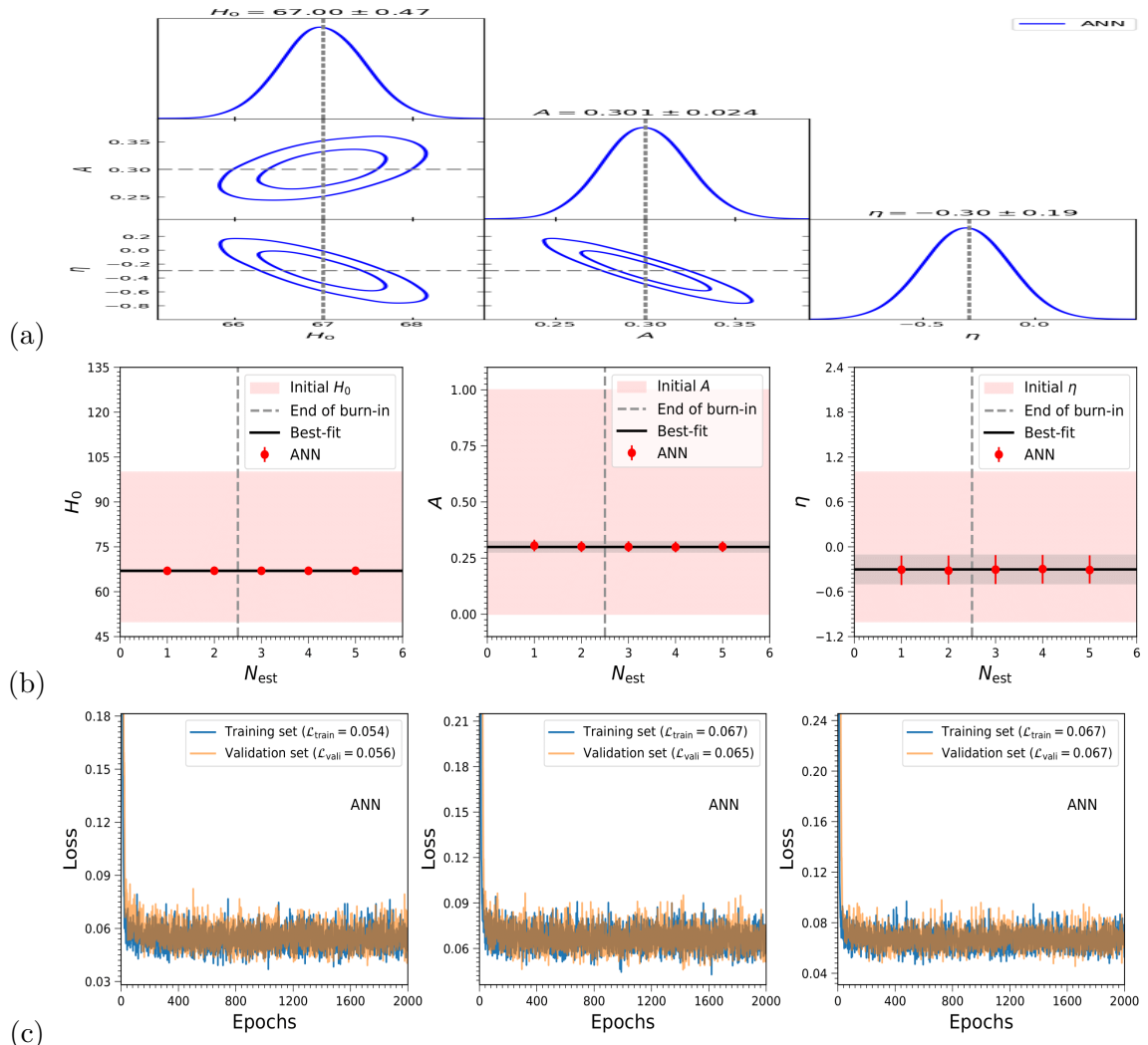


Figure 9. Observational analysis of the Rastall-gravity based cosmological model using ANN model: (a), (b), and (c) have their own description of legends as in the previous Fig. 3.

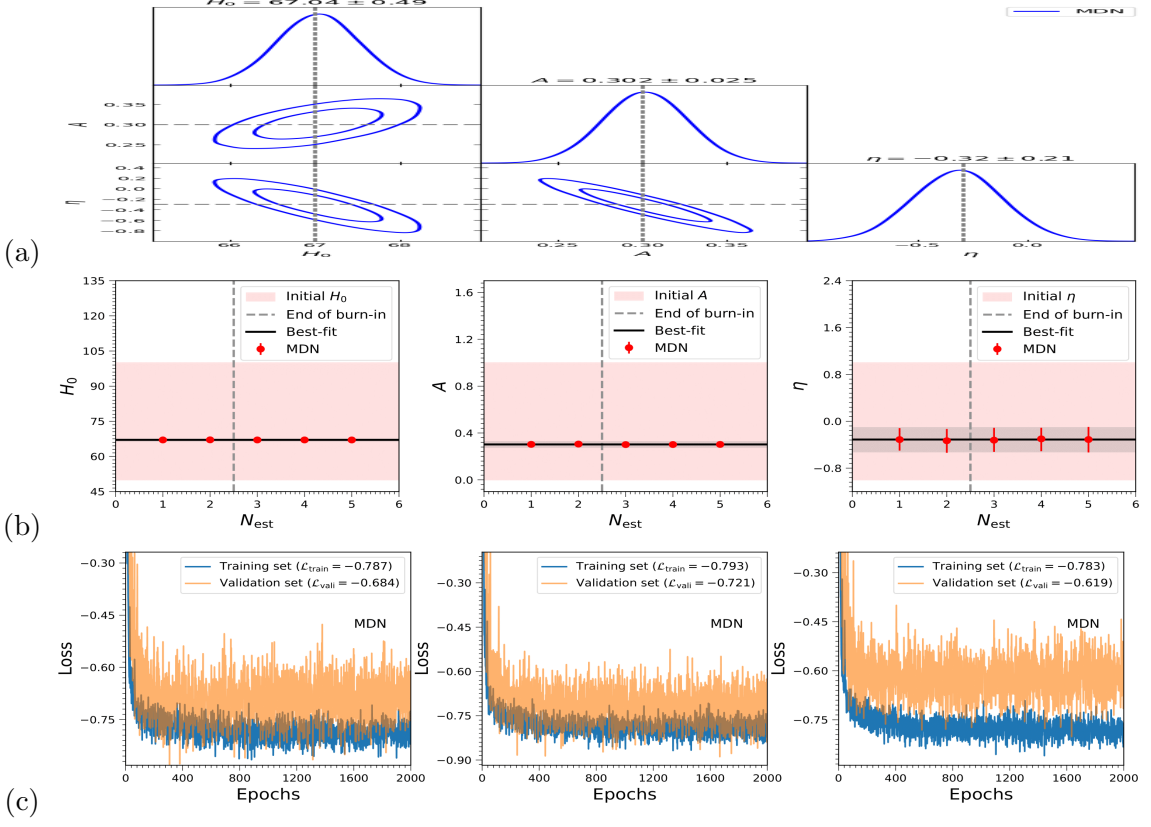


Figure 10. Observational analysis of the Rastall-gravity based cosmological model using MDN model: (a), (b), and (c) have their own description of legends as in the previous Fig. 3.

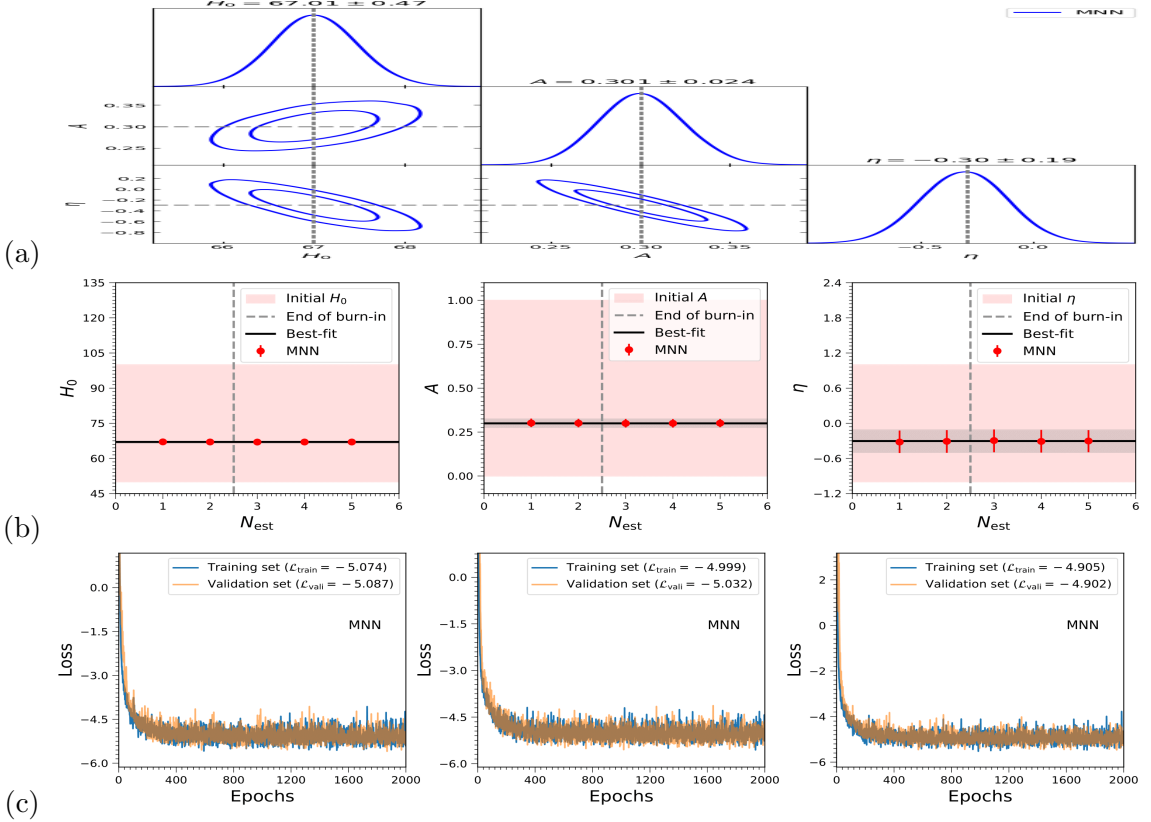


Figure 11. Observational analysis of the Rastall-gravity based cosmological model using MNN model: (a), (b), and (c) have their own description of legends as in the previous Fig. 3.

APPENDIX B

In this appendix, we describe the statefinder parameters (i.e., r and s), which are used to show Fig. 7. The explicit expressions are given by

$$\begin{aligned} r &= 2q^2 + q - \frac{\dot{q}}{H} \\ &= \{3A^2(z+1)^8 - 2A(z^2 + 2z - 2)(z+1)^3(3B - 2\eta) - 2\eta(z+1)^2 \log(z+1) \\ &\quad \times [3A(z^3 + 3z^2 - 2) + \eta] + \eta[\eta(z^2 + 2z - 1) - 2B(z+1)^2]\} \\ &\quad / \{4(z+1)^2 [A(z+1)^3 + B + \eta \log(z+1)]^2\}, \end{aligned} \quad (6.1)$$

$$\begin{aligned} s &= \frac{r-1}{3(q-\frac{1}{2})} \\ &= \{A^2(z+1)^8 + 2A(z+1)^3[B(7z^2 + 14z - 2) - 2\eta(z^2 + 2z - 2)] \\ &\quad + 2\eta(z+1)^2 \log(z+1)[A(7z^3 + 21z^2 + 12z - 2) + 4B + \eta] + 4B^2(1+z)^2 \\ &\quad + 2B\eta(1+z)^2 + \eta^2 - \eta^2 z^2 - 2\eta^2 z + 4\eta^2(z+1)^2 \log^2(z+1)\} \\ &\quad / \{6(z+1)^2[3B - \eta + 3\eta \log(z+1)][A(z+1)^3 + B + \eta \log(z+1)]\}. \end{aligned} \quad (6.2)$$

[1] A. G. Riess, et al., Observational evidence from supernovae for an accelerating universe and a cosmological constant, *Astron. J.* **116** (1998) 1009.

[2] S. Perlmutter, et al., Measurements of Ω and Λ from 42 high-redshift supernovae, *Astrophys. J.* **517** (1999) 565.

[3] C. L. Bennett et al., Nine-year Wilkinson Microwave Anisotropy Probe (WMAP) observations: final maps and results, *Astrophys. J. Suppl. Ser.* **208** (2013) 20.

[4] E. Komatsu et al., Five-year Wilkinson microwave anisotropy probe (WMAP) observations: cosmological interpretation, *Astrophys. J. Suppl.* **180** (2009) 330.

[5] L. Anderson et al., The clustering of galaxies in the SDSS-III Baryon Oscillation Spectroscopic Survey: Baryon acoustic oscillations in the Data Releases 10 and 11 Galaxy samples, *Mon. Not. R. Astron. Soc.* **441** (2014) 24–62.

[6] P. A. R. Ade et al., Planck 2015 results - XIII, cosmological parameters, *Astron. Astrophys.* **594** (2016) A13.

[7] M. Tegmark et al., Cosmological parameters from SDSS and WMAP, *Phys. Rev. D* **69** (2004) 103501.

[8] P. J. E. Peebles, and B. Ratra, The cosmological constant and dark energy, *Rev. Mod. Phys.* **75** (2003) 559.

[9] V. Sahni and A. Starobinsky, The Case for a positive cosmological Λ -term, *Int. J. Mod. Phys. D* **9** (2000) 373.

[10] R. R. Caldwell, A Phantom Menace? Cosmological consequences of a dark energy component with super-negative equation of state, *Phys. Lett. B* **545** (2002) 23–29.

[11] S. M. Carroll, M. Hoffman, and M. Trodden, Can the dark energy equation-of-state parameter ω be less than -1 ? *Phys. Rev. D* **68** (2003) 023509.

[12] T. P. Sotiriou, V. Faraoni, $f(R)$ theories of gravity, *Rev. Mod. Phys.* **82** (2010) 451.

[13] A. De Felice, S. Tsujikawa, $f(R)$ theories, *Liv. Rev. Rel.* **13** (2010) 1–161.

[14] S. Nojiri and S. D. Odintsov, Unified cosmic history in modified gravity: from $F(R)$ theory to Lorentz non-invariant models, *Phys. Rep.* **505** (2011) 59–144.

[15] G. R. Bengochea, R. Ferraro, Dark torsion as the cosmic speed-up, *Phys. Rev. D* **79** (2009) 124019.

[16] E. V. Linder, Einstein's other gravity and the acceleration of the universe, *Phys. Rev. D* **81** (2010) 127301.

[17] V. Faraoni and S. Capozziello, Beyond Einstein gravity: a survey of gravitational theories for cosmology and astrophysics, Springer Netherlands (2011).

[18] T. Clifton et al., Modified gravity and cosmology, *Phys. Rep.* **513** (2012) 1-189.

[19] L. Parker, Quantized fields and particle creation in expanding universes. II, *Phys. Rev. D* **3** (1971): 346.

[20] G. W. Gibbons and S. W. Hawking. "Cosmological event horizons, thermodynamics, and particle creation, *Phys. Rev. D* **15** (1977) 2738.

[21] N. D. Birrell and P. C. W. Davies, *Quantum fields in curved space*, Cambridge Univ. Press (2012), DOI: <https://doi.org/10.1017/CBO9780511622632>.

[22] L. H. Ford, Gravitational particle creation and inflation, *Phys. Rev. D* **35** (1987) 2955.

[23] S. Capozziello and M. D. Laurentis, Extended theories of gravity, *Phys. Rep.* **509** (2011) 167-321.

[24] C. M. Will, The confrontation between general relativity and experiment, *Liv. Rev. Relativ.* **17** (2014) 1-117.

[25] S. Nojiri, S. D. Odintsov, V. K. Oikonomou, Modified gravity theories on a nutshell: Inflation, bounce and late-time evolution, *Phys. Rep.* **692** (2017) 1.

[26] A. G. Riess et al., The farthest known supernova: support for an accelerating universe and a glimpse of the epoch of deceleration, *Astrophys. J.* **560** (2001) 49.

[27] J. F. Navarro, C. S. Frenk and S. D. M. White, A universal density profile from hierarchical clustering, *Astrophys. J.* **490** (1997) 493.

[28] D. Clowe et al., A direct empirical proof of the existence of dark matter, *Astrophys. J.* **648** (2006) L109.

[29] T. Harko, F.S.N. Lobo, S. Nojiri, S.D. Odintsov, $f(R, T)$ gravity, *Phys. Rev. D* **84** (2011) 024020.

[30] J. K. Singh et al., EDSFD parameterization in $f(R, T)$ gravity with linear curvature terms, *Phys. Dark Univ.* **45** (2024) 101513.

[31] L. K. Sharma et al., Constraining anisotropic universe under $f(R, T)$ theory of gravity, *J. High Ener. Astrophys.* **44** (2024) 457-467.

[32] V. K. Bhardwaj, Non-minimal matter-geometry coupling in the Bianchi-V spacetime within the formalism of $f(R, T) = f_1(R) + f_2(R)f_3(T)$ cosmology, *Mod. Phys. Lett. A* **33** (2018) 1850234.

[33] H. Shabani and A. H. Ziaie, Stability of the Einstein static universe in $f(R, T)$ gravity, *Eur. Phys. J. C* **77** (2017) 1-15.

[34] V. K. Bhardwaj, P. Garg, and S. Prakash, Cosmological dynamics of accelerating model in $f(Q)$ gravity with latest observational data, *Astrophys. Space Sci.* **369** (2024) 50.

[35] J. K. Singh et al., Bouncing cosmology in modified gravity with higher-order curvature terms, *J. High Ener. Phys.* **2023** (2023) 1-21.

[36] P. Rastall, Generalization of the Einstein theory, *Phys. Rev. D* **6** (1972) 3357.

[37] C. E. M. Batista et al., Rastall cosmology and the Λ CDM model, *Phys. Rev. D* **85** (2012) 084008.

[38] S. Nojiri and S.D. Odintsov, Gravity assisted dark energy dominance and cosmic acceleration, *Phys. Lett. B* **599** (2004) 137-142.

[39] T. Koivisto, A note on covariant conservation of energy-momentum in modified gravities, *Class. Quantum Gravit.* **23** (2006) 4289.

[40] O. Bertolami et al., Extra force in $f(R)$ modified theories of gravity, *Phys. Rev. D* **75** (2007) 104016.

[41] T. Harko and F. S. N. Lobo, Generalized curvature-matter couplings in modified gravity, *Galaxies* **2** (2014) 410-465.

[42] A. H. Ziaie, H. Shabani, and S. Ghaffari, Effects of Rastall parameter on perturbation of dark sectors of the Universe, *Mod. Phys. Lett. A* **36** (2021) 2150082.

[43] T. R. P. Carames et al., The brans-dicke-rastall theory, *Eur. Phys. J. C* **74** (2014) 3145.

[44] S. K. Maurya and F. Tello-Ortiz, Decoupling gravitational sources by MGD approach in Rastall gravity, *Phys. Dark Univ.* **29** (2020) 100577.

[45] J. C. Fabris, M. H. Daouda, and O. F. Piattella, Note on the evolution of the gravitational potential in Rastall scalar field theories, *Phys. Lett. B* **711** (2012) 232-237.

[46] A. Singh and K. C. Mishra, Aspects of some Rastall cosmologies, *Eur. Phys. J. Plus* **135** (2020) 752.

[47] J. K. Singh et al., Evolution of the Universe with quintessence model in Rastall gravity, *Phys. Scrip.* **99** (2024) 125001.

[48] C. E. M. Batista et al., Observational constraints on Rastall's cosmology, *Eur. Phys. J. C* **73** (2013) 1-7.

[49] K. Lin and W. L. Qian, Cosmic evolution of dark energy in a generalized Rastall gravity, *Eur. Phys. J. C* **80** (2020) 1-8.

[50] J. C. Fabris, R. Kerner, and J. Tossa, Perturbative analysis of generalized Einstein theories, *Int. J. Mod. Phys. D* **9** (2000) 111-125.

[51] H. Moradpour et al., A generalization to the Rastall theory and cosmic eras, *Eur. Phys. J. C* **77** (2017) 1-9.

[52] D. Das, S. Dutta, and S. Chakraborty, Cosmological consequences in the framework of generalized Rastall theory of gravity, *Eur. Phys. J. C* **78** (2018) 1-8.

[53] W. Khyllep and J. Dutta, Linear growth index of matter perturbations in Rastall gravity, *Phys. Lett. B* **797** (2019) 134796.

[54] M. Visser, Rastall gravity is equivalent to Einstein gravity, *Phys. Lett. B* **782** (2018) 83-86.

[55] A. Golovnev, More on the fact that Rastall = GR, *Ann. Phys.* **461** (2024) 169580.

[56] F. Darabi, H. Moradpour, I. Licata, Y. Heydarzade, and C. Corda, Einstein and Rastall Theories of Gravitation in Comparison, *Eur. Phys. J. C* **78** (2018) 25.

[57] G. Abbas, M. R. Shahzad, Comparative analysis of Einstein gravity and Rastall gravity for the compact objects, *Chin. J. Phys.* **63** (2020) 1-12.

[58] J. Chagoya, J. C. López-Domínguez, and C. Ortiz, Cosmological fluids in the equivalence between Rastall and Einstein gravity, *Class. Quant. Grav.* **40** (2023) 075005.

[59] G. J. Wang et al., CoLFI: Cosmological Likelihood-free Inference with Neural Density Estimators, *Astrophys. J. Suppl.* **268** (2023) 7.

[60] R. Al-Rfou, A. G. Alain, A. Almahairi, et al. (The Theano Development Team), Theano: A Python framework for fast computation of mathematical expressions, *arXiv:1605.02688* (2016).

[61] G. J. Wang, S. Y. Li, and J. Q. Xia, ECoPANN: A Framework for Estimating Cosmological Parameters using Artificial Neural Networks, *Astrophys. J. Suppl.* **249** (2020) 25

[62] G. J. Wang, C. Cheng, Y. Z. Ma, and J. Q. Xia, Likelihood-free Inference with the Mixture Density Network, *Astrophys. J. Suppl.* **262** (2022) 24.

[63] L. K. Sharma et al., A comprehensive analysis of observational cosmology in $f(Q)$ gravity with deep learning and MCMC method, *Astron. Comput.* **49** (2024) 100892.

[64] S. Perlmutter et al. (Supernova Cosmology Project), Measurements of Ω and Λ from 42 high redshift supernovae, *Astrophys. J.* **517** (1999) 565-86.

[65] A. G. Riess et al. (Supernova Search Team), Observational evidence from supernovae for an accelerating Universe and a cosmological constant, *Astron. J.* **116** (1998) 1009-1038.

[66] Y. Akrami et al. (Planck Collaboration), Planck 2018 results. I. Overview, and the cosmological legacy of Planck, *Astron. Astrophys.* **641** (2020) A1.

[67] N. Aghanim et al. (Planck Collaboration), Planck 2018 results V. CMB power spectra and likelihoods, *Astron. Astrophys.* **641** (2020) A5.

[68] G. Hinshaw et al., Five-year Wilkinson Microwave Anisotropy Probe observations: Data processing, sky maps, and basic results, *Astrophys. J. Suppl. Ser.* **180** (2009) 225-245.

[69] C. L. Bennett et al., Nine-Year Wilkinson Microwave Anisotropy Probe (WMAP) Observations: Final Maps and Results, *Astrophys. J. Suppl. Ser.* **208** (2012) 20.

[70] S. M. Carroll, J. Chen, Spontaneous Inflation and the Origin of the Arrow of Time, *arXiv:hep-th/0410270*.

[71] A. L. Coil, The Large-Scale Structure of the Universe, Planets, Stars and Stellar Systems, pp. 387-421 (2013).

[72] S. Pradhan, G. N. Gadbail, S. Mandal, P. K. Sahoo, and K. Bamba, Dynamics of interacting dark energy and dark matter model in a curved FLRW scalar field cosmology, *Mon. Not. R. Astron. Soc.* **543** (2025) 1273-1287.

[73] M. Capone, V. F. Cardone, and M. L. Ruggiero, Accelerating Cosmology in Rastall's Theory, *Nuo. Cim. B* **125** (2011) 1133-1142.

[74] A. Shafieloo, A. G. Kim, and E. V. Linder, Model independent tests of cosmic growth versus expansion, *Phys. Rev. D* **87** (2013) 2.

[75] V. Sahni, T. D. Saini, A. A. Starobinsky, and U. Alam, Statefinder-A new geometrical diagnostic of dark energy, *J. Exp. Theor. Phys. Lett.* **77** (2003) 201.

[76] C. Escamilla-Rivera, A. Najera, Dynamical dark energy models in the light of gravitational-wave transient catalogues, *J. Cosmol. Astropart. Phys.* **2022** (2022) 03.

[77] J. V. Cunha and J. A. S. Lima, Transition redshift: new kinematic constraints from supernovae, *Mon. Not. Roy. Astr. Soc.* **390** (2008) 210.

[78] S. K. J. Pacif, Dark energy models from a parametrization of H: a comprehensive analysis and observational constraints, *Eur. Phys. J. Plus* **135** (2020) 10.

[79] S. Myrzakulova, M. Koussour, and N. Myrzakulov, Investigating the dark energy phenomenon in $f(R, L_m)$ cosmological models with observational constraints, *Phys. Dark Univ.* **43** (2024) 101399.

[80] S. Capozziello et al., Cosmographic bounds on the cosmological deceleration-acceleration transition redshift in $f(R)$ gravity, *Phys. Rev. D* **90** (2014) 044016.

[81] P. Lemos et al., Model independent $H(z)$ reconstruction using the cosmic inverse distance ladder, *Mon. Not. R. Astron. Soc.* **483** (2019) 4803-4810.

[82] H. Yu, B. Ratra, F.-Y. Wang, Hubble Parameter and Baryon Acoustic Oscillation Measurement Constraints on the Hubble Constant, the Deviation from the Spatially Flat Λ CDM Model, the Deceleration-Acceleration Transition Redshift, and Spatial Curvature, *Astrophys. J.* **856** (2018) 3.

[83] M. Moresco, Raising the bar: new constraints on the Hubble parameter with cosmic chronometers at $z \sim 2$, *Mon. Not. R. Astron. Soc.* **450** (2015) L16–L20.

[84] D. M. Scolnic et al., The Complete Light-curve Sample of Spectroscopically Confirmed SNe Ia from Pan-STARRS1 and Cosmological Constraints from the Combined Pantheon Sample, *Astrophys. J.* **859** (2018) 101.

[85] D. Brout, G. Taylor, D. Scolnic et al. The Pantheon+ Analysis: SuperCal-Fragilistic Cross Calibration, Retrained SALT2 Light Curve Model, and Calibration Systematic Uncertainty, *Astrophys. J.* **938** (2022) 111.

[86] C. Blake et al., The WiggleZ Dark Energy Survey: mapping the distance-redshift relation with baryon acoustic oscillations, *Mon. Not. R. Astron. Soc.* **418** (2011) 1707.

[87] W. J. Percival et al., Baryon Acoustic Oscillations in the Sloan Digital Sky Survey Data Release 7 Galaxy Sample, *Mon. Not. R. Astron. Soc.* **401** (2010) 2148.

[88] F. Beutler et al., The 6dF Galaxy Survey: baryon acoustic oscillations and the local Hubble constant, *Mon. Not. R. Astron. Soc.* **416** (2011) 3017.

[89] R. Giostri et al., From cosmic deceleration to acceleration: new constraints from SN Ia and BAO/CMB, *J. Cosmol. Astropart. Phys.* **2012** (2012) 027.

[90] A. A. Mamon, K. Bamba, and S. Das, Constraints on reconstructed dark energy model from SN Ia and BAO/CMB observations, *Eur. Phys. J. C* **77** (2017) 29.

[91] S. Capozziello et al., Thermodynamic parametrization of dark energy, *Mon. Not. R. Astron. Soc.* **509** (2022) 5399.

[92] M. Muccino, O. Luongo, and D. Jain, Constraints on the transition redshift from the calibrated gamma-ray burst E_p -Eiso correlation, *Mon. Not. R. Astron. Soc.* **523** (2023) 4938.

[93] D. Rubin et al., Union through UNITY: Cosmology with 2000 SNe Using a Unified Bayesian Framework, *Astrophys. J.* **986** (2025) 231.

[94] I. Tutusaus, B. Lamine, A. Blanchard, Model-independent cosmic acceleration and redshift-dependent intrinsic luminosity in type-Ia supernovae, *Astron. Astrophys.* **625** (2019) A15.

[95] G. Benevento, W. Hu, and M Raveri, Can late dark energy transitions raise the Hubble constant? *Phys. Rev. D* **101** (2020) 103517.

[96] L. Chen, Q. G. Huang, and K. Wang, Distance priors from Planck final release, *J. Cosmo. Astropart. Phys.* **2019** (2019) 028.

[97] N. Aghanim et al. (Planck), Planck 2018 results. V. CMB power spectra and likelihoods, *Astron. Astrophys.* **641** (2020) A5.

[98] A. G. Adame et al., DESI 2024 VI: cosmological constraints from the measurements of baryon acoustic oscillations, *J. Cosmo. Astropart. Phys.* **2025** (2025) 021.

[99] K. Lodha et al. (DESI collaboration), Extended Dark Energy analysis using DESI DR2 BAO measurements, *Phys. Rev. D* **112** (2025) 083511.

[100] M. A. Karim et al. (DESI collaboration), DESI DR2 results II: Measurements of baryon acoustic oscillations and cosmological constraints, *Phys. Rev. D* **112** (2025) 083515.

[101] M. V. D. Santos et al., Constraining the cosmic deceleration-acceleration transition with type Ia supernova, BAO/CMB and $H(z)$ data, *J. Cosmo. Astropart. Phys.* **2016** (2016) 066.

[102] S. Masi et al., The BOOMERanG experiment and the curvature of the Universe, *Prog. Part. Nucl. Phys.* **48** (2002) 243.

[103] V. K. Bhardwaj, S. Prakash, Observational constraints on anisotropic cosmological model in Lyra's manifold, *Chin. J. Phys.* **87** (2024) 665.

[104] O. Farooq, B. Ratra, Hubble parameter measurement constraints on the cosmological deceleration-acceleration transition redshift, *Astrophys. J. Lett.* **766** (2013) L7.

[105] U. Alam, V. Sahni, T. Deep Saini, A. A. Starobinsky, Exploring the expanding universe and dark energy using the Statefinder diagnostic, *Mon. Not. Roy Astron Soc.* **344** (2003) 1057.

[106] X. Zhang, Statefinder diagnostic for holographic dark energy model, *Int. J. Mod. Phys D* **14** (2005) 1597.

[107] M. R. Setare, J. Zhang, X. Zhang, Statefinder diagnosis in a non-flat universe and the holographic model of dark energy, *J. Cosmol. Astropart. Phys.* **3** (2007) 007.

[108] V. K. Bhardwaj, A. K. Yadav, Observation constraints on scalar field cosmological model in Anisotropic universe, *Int. J. Geom. Meth. Mod. Phys.* **21** (2024) 2450144.

[109] J. Santos, J. S. Alcaniz, Energy conditions and Segre classification of phantom fields, *Phys. Lett. B* **619** (2005) 11.

[110] J. Santos et al., Energy conditions in $f(R)$ gravity, *Phys. Rev. D* **76** (2007) 083513.

[111] S. M. Carroll, *Spacetime and Geometry: An Introduction to General Relativity*, Addison Wesley, Boston (2004).

[112] S. Capozziello, S. Nojiri, and S. D. Odintsov, The role of energy conditions in $f(R)$ cosmology, *Phys. Lett. B* **781** (2018) 99-106.

[113] V. K Bhardwaj, M. K. Rana, and A. K Yadav, Bulk viscous Bianchi-V cosmological model within the formalism of $f(R, T) = f_1(R) + f_2(R)f_3(T)$ gravity, *Astrophys. Space Sci.* **364** (2019) 1.

[114] E. J. Copeland, M. Sami, and S. Tsujikawa, Dynamics of dark energy, *Int. J. Mod. Phys. D* **15** (2006) 1753.

[115] B. Ratra, P. J. E. Peebles, Cosmological consequences of a rolling homogeneous scalar field, *Phys. Rev. D* **37** (1988) 3406.

[116] B. S. Jayas, V. K. Bhardwaj, Evaluation of transit cosmological model in $f(R, T^\phi)$ theory of gravity, *Int. J. Mod. Phys. A* **39** (2024) 2450106.

[117] T. N. Li, Y. H. Li, G. H. Du, P. J. Wu, L. Feng, J. F. Zhang, and X. Zhang, “Revisiting holographic dark energy after DESI 2024”, *Eur. Phys. J. C* **85** (2025) 608.

[118] M. Lopez-Hernandez, J. De-Santiago, Is there a dynamical tendency in H_0 with late time measurements? *JCAP* **03** (2025) 026.

[119] W. Guo et al., Newest measurements of Hubble constant from DESI 2024 BAO observations, arXiv:2412.13045 [astro-ph.CO]

[120] D. Kumar, D. Jain, and S. Mahajan, A cosmographic analysis using DESI- DR2 and strong lensing: I. Time-Delay measurements, arXiv:2511.00788v1 [astro-ph.CO].

[121] M. A. Sabogal, R. C. Nunes, F. Avila, and A. Bernui, Updated Cosmological Constraints from 2D BAO Measurements: A New Compilation and Comparison with DESI DR2, arXiv:2510.16141v1 [astro-ph.CO].

[122] C. Zhang, H. Zhang, S. Yuan et al., Four new observational $H(z)$ data from luminous red galaxies in the Sloan Digital Sky Survey data release seven, *Res. Astron. Astrophys.* **14** (2014) 1221.

[123] J. Simon, L. Verde, and R. Jimenez, Constraints on the redshift dependence of the dark energy potential, *Phys. Rev. D* **71** (2005) 123001.

[124] M. Moresco, A. Cimatti, R. Jimenez et al., Improved constraints on the expansion rate of the Universe up to $z \sim 1.1$ from the spectroscopic evolution of cosmic chronometers, *JCAP* **1208** (2012) 006.

[125] S. Alam et al., The clustering of galaxies in the completed SDSS-III Baryon Oscillation Spectroscopic Survey: cosmological analysis of the DR12 galaxy sample, *Mon. Not. R. Astron. Soc.* **470** (2017) 2617–2652.

- [126] M. Moresco, L. Pozzetti, A. Cimatti et al., A 6% measurement of the Hubble parameter at : direct evidence of the epoch of cosmic re-acceleration, *JCAP* **1605** (2016) 014.
- [127] A. L. Ratsimbazafy, S. I. Loubser, S. M. Crawford et al., Age-dating Luminous Red Galaxies observed with the Southern African Large Telescope, *Mon. Not. R. Astron. Soc.* **467** (2017) 3239.
- [128] M. Moresco, Raising the bar: new constraints on the Hubble parameter with cosmic chronometers at $z \sim 2$, *Mon. Not. R. Astron. Soc.* **450** (2015) L16.